Progress In Electromagnetics Research C, Vol. 58, 169–181, 2015

A Novel Wide Band Microstrip-Line-Fed Antenna with Defected Ground for CP Operation

Jamshed A. Ansari[1], Sapna Verma[1, *], Mahesh K. Verma[2], and Neelesh Agrawal[3]

Abstract—A novel wide band microstrip line-fed antenna with defected ground structure is proposed for circularly polarized characteristics. This antenna is suitable for C-band and partially X-band operation. Antenna1 structure consists of microstrip-line-feed, and the square-shaped slot defect is incorporated in the ground plane. Furthermore, rectangular and circular patches are embedded in the square-shaped slot that improves the performance of the radiating Antenna2 and Antenna3 structures, respectively. The proposed Antenna3 is compact in size and shows a good quality of polarization at resonant frequency band. Antenna3 shows the measured impedance bandwidth of 40.72% (6.45–9.75 GHz) and also shows the variations of 3-dB axial ratio bandwidth at the 6.806 GHz and 9.13 GHz frequencies with the simulated results, respectively. The return loss, axial ratio, gain, efficiency and radiation pattern of the proposed Antenna3 remain consistent for resonant frequency band. The antenna is practically fabricated and simulated. Measured result shows a good agreement with simulated and theoretical ones.

1. INTRODUCTION

Nowadays the rapid development of modern communication systems are required for portable devices due to some important features including easy design, light in weight, reduction in size, compatibility with microwave, millimeter-wave integrated circuits, low production cost [1] and easy fabrication of microstrip antennas. DGS antennas are particularly attractive because of their miniaturized size, wide impedance bandwidth, good gain and better efficiency. Furthermore, broadband microstrip antennas are developed for the high-speed data communication systems which are achieved at higher frequency bands. However, these conventional microstrip antennas exhibit a few major limitations such as narrow impedance bandwidth and low gain, which restrict their operation while enhancement of the bandwidth and gain of the microstrip patch antenna has become a demanding current research area. Recently, a growing demand of the microstrip patch antennas with modified ground structure has been rapidly developed for broadband and dual-frequency band in the wide range of modern communication systems.

Hence, several researchers have reported numerous techniques to improve the performance of the patch antenna with modified ground plane such as I-shaped slotted patch antenna for WLAN/WiMAX applications [2], asymmetric slit antenna for circular polarization operation [3, 4], concentric circular-ring shaped [5], dual inverted L-shaped strips microstrip-fed monopole antenna which consists of rectangular patch [6], triple band antenna using Y-shaped strip in circular ring with defected ground antenna [7], slotted microstrip antenna [8], monopole antenna with two strips for triple band operation and I-shaped microstrip line used to excite wide-slot antenna [9, 10]. The dumbbell-shaped DGS antenna incorporated with CSRR for dual-bandgap characteristics and microstrip-line-fed antenna with defected ground structure are used for Ku-band application which gives a better impedance bandwidth and

Received 23 May 2015, Accepted 25 June 2015, Scheduled 30 July 2015
* Corresponding author: Sapna Verma (sverma.ece@gmail.com).
[1] Department of Electronics and Communication, University of Allahabad, Allahabad 211002, India. [2] Uttar Pradesh Technical University, Lucknow 226021, India. [3] Sam Higginbottom Institute of Agriculture Technology & Science, Allahabad 211007, India.

gain [11, 12]. A $32 \times 32\,\text{mm}^2$ size Z-shaped metal strip removed from the ground plane to enhance the bandwidth upto 12.2% [13], compact broadband microstrip antenna with defected ground structure was proposed in [14]. A dual ultrawide band slotted antenna with gain 5.54 dBi and an inverted S-shaped compact antenna [15, 16] were reported for the C- and X-band applications and compared with the proposed antenna in Table 4. Hence, in several reported research techniques a lot of modified types of microstrip antennas have been suggested so far. However, the microstrip patch antenna which is especially realized on the single substrate layer has a significant drawback of very narrow bandwidth, 1–5%. To overcome this disadvantage, there have been a number of methods as broadband techniques such as using multilayer, stacked antennas structure for coaxial probe, slot and aperture coupled feeding [17]. However, these antennas are still not large enough, and their structures are too complex, with narrow bandwidth and low gain. The concept of the proposed antenna structure has been extracted from [12] which gives a good impedance bandwidth and gain discussed above.

In this article, a novel microstrip-line-fed printed antenna with defected ground structure has been proposed for C-band and partially X-band operation. A square slot and a circular patch are integrated in the ground plane. It provides a significant size reduction and large impedance bandwidth with circular polarization characteristics. The analysis of the proposed Antenna3 is carried out using circuit theory concept based on modal expansion cavity model. A parametric study has been carried out by varying the length, width of the microstrip-fed-line and radius of the circular patch. Various parameters such as return loss, axial ratio, gain, efficiency and radiation pattern of the proposed antenna have been investigated. The details are discussed in the following section.

2. ANTENNA DESIGN

Figure 1 illustrates the configuration of the proposed microstrip-line-fed antenna with defected ground structure. The proposed antenna is fabricated on an inexpensive FR4 dielectric substrate with relative permittivity $\varepsilon_r = 4.4$, thickness $h = 1.6\,\text{mm}$ and dielectric loss tangent $\tan\delta = 0.02$. The main radiating elements of the antenna are printed on the bottom of the substrate which consists of a circle incorporated in the centre of square slot. The square slot dimension is $14.5 \times 14.5\,\text{mm}^2$ and radius of the circle 7.0 mm. The antenna is fed by a $50\,\Omega$ microstrip-line-fed with a width 3.05 mm and length 22.55 mm. The square ground plane is located on the backside of the dielectric substrate with the overall dimensions of $32 \times 32\,\text{mm}^2$ [see Figure 1(b)]. A square patch is replaced by circular patch defect in the ground plane under the square shaped slot and makes Antenna3 structure which achieves a better impedance matching. The gap between the square shaped slot and a circular patch affects the antenna performance. Detailed design specifications of the proposed Antenna3 are optimized and shown in Table 1.

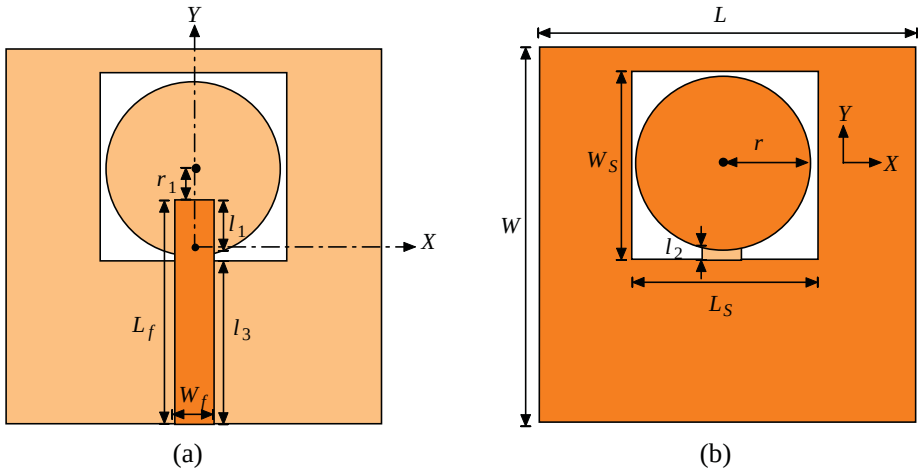

Figure 1. Proposed antenna geometry. (a) Top view. (b) Bottom view.

Table 1. Design specifications of the proposed antenna.

Parameter name	ε_r	$\tan\delta$	h	L_f	W_f	l_1
Parameter value	4.4	0.02	1.6 (mm)	22.55 (mm)	3.05 (mm)	6.45 (mm)
Parameter name	l_2	l_3	L_s	W_s	r	r_1
Parameter value	0.5 (mm)	15.60 (mm)	145 (mm)	145 (mm)	7.0 (mm)	0.5 (mm)

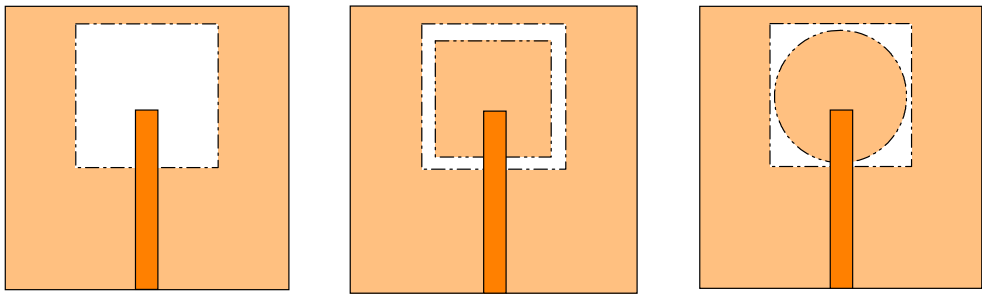

Figure 2. Evolution steps of the wide band antenna with defected ground structure. (a) Antenna1. (b) Antenna2. (c) Proposed Antenna3.

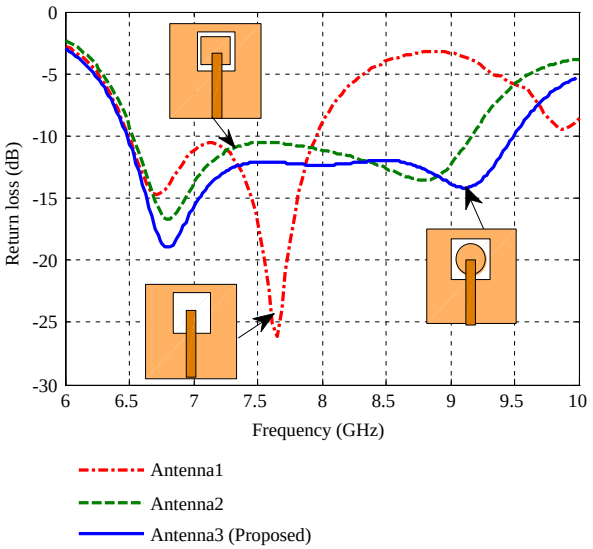

Figure 3. Comparative plot of simulated return loss versus frequency for Antenna1, Antenna2 and proposed Antenna3.

3. EVOLUTION PROCESS OF THE PROPOSED ANTENNA

This section presents the description of evolution process for the proposed antenna with defected ground structure. Different steps in the evolution process of the proposed antenna and its corresponding simulated return losses are shown in Figures 2 and 3. It begins with the design of Antenna1, which consists of a square-shaped slot with the dimension of $14.5\times14.5\,\text{mm}^2$ as shown in Figure 2(a). Antenna1 obtains the impedance bandwidth 20.06 % (6.5–7.95 GHz) at the dual resonance frequencies 6.711 GHz and 7.65 GHz as shown in Figure 3. Antenna2 is created by incorporating the rectangular patch with the dimension of $14.0\times14.0\,\text{mm}^2$ under the square-shaped slot on the ground plane as shown in Figure 2(b),

and its corresponding bandwidth is 33.12% (6.55 GHz–9.15 GHz) at the 6.795 GHz and 8.771 GHz dual resonance frequencies (see Figure 3). It is worth mentioning that the defected ground structure also affects the antenna characteristics. In this proposed design, a circular patch is etched in the square-shaped slot in place of rectangular patch under the ground plane to achieve good impedance performance during the operating frequency band and keep the wide band at the same time. Antenna1, Antenna2 and proposed Antenna3 have good impedance matching at the lower resonance frequencies, but at the higher resonance, the frequencies are shifted towards the upper side as shown in Figure 3. Finally, the proposed antenna has impedance bandwidth of 37.79% (6.48 GHz–9.5 GHz) at the 6.806 GHz and 9.13 GHz dual resonance frequencies.

The comparative curve for return loss versus frequency of the Antenna1, Antenna2 and Antenna3 is shown in Figure 3. From the figure, the impedance bandwidths of Antenna1 (20.06%), Antenna2 (33.12%) and Antenna3 (37.79%) are noticed. From these results, it is observed that Antenna3 achieves a better impedance bandwidth compared to Antenna1 and Antenna2. Thus, the proposed wideband Antenna3 can be used for C-band and partially X-band applications.

4. THEORETICAL ANALYSIS OF PROPOSED ANTENNA

The theoretical analysis of the proposed Antenna3 is done by equivalent circuit theory approach. The length (L_f) of the microstrip line is subdivided into three sections l_1, l_2 and l_3. There is no ground plane under length l_2. Length l_3 of the microstrip line works as a stub matching for the defected ground plane. Length L_f of the microstrip line can be calculated as [17]

$$L_f = l_1 + l_2 + l_3 = \frac{5}{4}\lambda_e \tag{1}$$

where

$$\lambda_e = \frac{c}{f\sqrt{\varepsilon_e}}$$

In which c = speed of light in free space and ε_e = effective dielectric constant [18]. Length L_f and width W_f of the microstrip line can be determined as 22.55 mm and 3.05 mm, respectively, for accurate matching.

A microstrip-line-feed works as a tuning stub which is used to excite the square-shaped slot and circular patch under the ground plane. The variation in the length and width of the stub affects the antenna characteristics. The discontinuity is added to the microstrip line and modelled by a fringing capacitance C_f. The distance 'r' is chosen as input impedance of the circular patch in the square slot is 50 Ω at the end-edge point of microstrip line for proper matching [19].

$$Z\ (r_1) = \frac{1}{G_T} \cdot \frac{J_1^2\,(k \cdot r_1)}{J_1^2\ (k \cdot r)} \tag{2}$$

where k is the propagation constant, r_1 the feed position referred to the center to the circular disk radius r, G_T the total conductance [18], and J_1 the Bessel function of order one [19].

The equivalent circuit is the combination of four parts: modelling of lengths l_1, l_2 and l_3 of microstrip line, square shaped slot, coupling capacitance C_f due to discontinuity of microstrip line and coupling capacitance C_p between the square slot and microstrip line. Both mutual inductance L_m

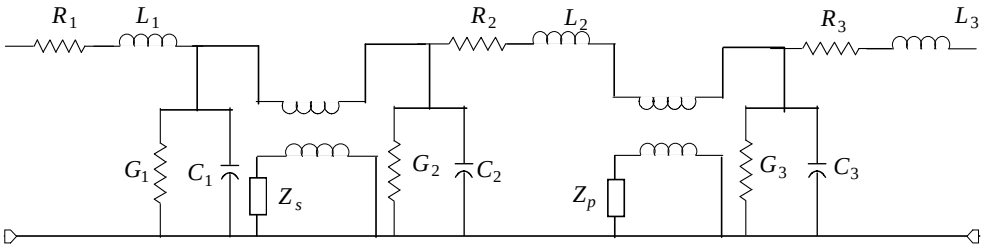

Figure 4. Equivalent circuit of DGS with microstrip line.

and mutual capacitance C_m between the square shaped slot and circular patch are under the ground plane. The total impedance of square slot and circular patch is modelled by an ideal transformer with the microstrip line, as shown in Figure 4. A microstrip line is represented by combination of circuit parameters such as series resistance (R), inductance (L), shunt conductance (G) and capacitance (C) and calculated for microstrip line. R_1, L_1, G_1, C_1, R_2, L_2, G_2, C_2 and R_3, L_3, G_3, C_3 parameters are equivalent to the microstrip line of lengths l_1, l_2 and l_3, respectively.

Series resistance (R) and Shunt conductance (G) are calculated as [19]

$$G = \frac{2 \cdot \alpha_d}{Z_0} \tag{3}$$

$$R = 2 \cdot \alpha_c \cdot Z_0 \tag{4}$$

Capacitance of the microstrip line can be calculated as [18]

$$C = \begin{cases} \dfrac{2\,\pi\,\varepsilon_0}{\ln\left(\dfrac{8h}{W_f} + \dfrac{W_f}{4h}\right)} & \text{for } \dfrac{W_f}{h} \leq 1 \\ \varepsilon_0\,\varepsilon_e \left[\dfrac{W_f}{h} + 1.393 + 0.667 \ln\left(\dfrac{W_f}{h} + 1.444\right)\right] & \text{for } \dfrac{W_f}{h} \geq 1 \end{cases} \tag{5}$$

Inductance of the microstrip line can be defined as [20]

$$L = \frac{1}{j\omega}\left[Z_0^2 \cdot (G + j\omega\, C) - R\right] \tag{6}$$

where α_d = dielectric loss, α_c = conductor loss, and Z_0 = characteristics impedance of the microstrip line (50 ohm).

4.1. Analysis of Square Slot and Circular Patch

Theoretically, the effect of the etched square shaped slot on ground plane can be approximately obtained by the impedance of a short dipole via well-known Babinet's principle [21, 22] given as

$$Z_s = \frac{\eta_0^2}{4Z_{dipole}} \tag{7}$$

where

$$Z_{dipole} \approx f_1(\beta l) - j\left(120\left(\ln\frac{2L_s}{W_s} - 1\right)\cot(\beta l) - f_2(\beta l)\right)$$

$$f_1(\beta l) = -0.4787 + 7.3246(\beta l) + 0.3963(\beta l)^2 + 15.613(\beta l)^3$$

$$f_2(\beta l) = -0.4456 + 17.0082(\beta l) - 8.6793(\beta l)^2 + 9.6031(\beta l)^3$$

The radius (r) of the circular patch can be determined as [23]

$$r = \frac{F}{\left\{1 + \dfrac{2h}{\pi\varepsilon_r F}\left[\ln\left(\dfrac{\pi F}{2h}\right) + 1.7726\right]\right\}^{1/2}} \tag{8}$$

where $\eta_0 = 120\pi$, L_s = length of the square slot, W_s = width or diameter of the square slot and

$$F = \frac{8.791 \times 10^9}{f\sqrt{\varepsilon_r}}$$

in which f = design frequency. The design frequency is considered as 6.5 GHz of the wideband proposed microstrip antenna for C-band and partially X-band applications.

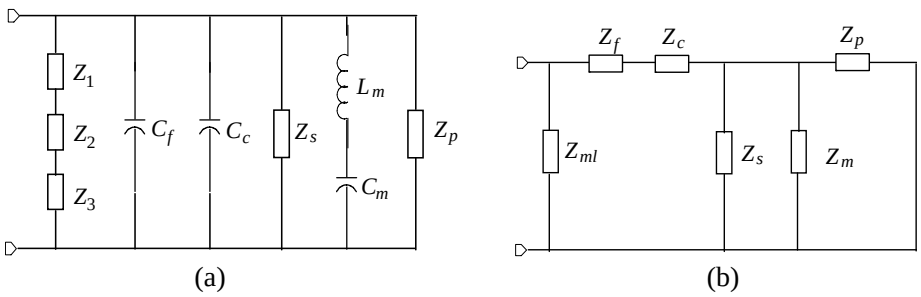

Figure 5. (a) Equivalent circuit model of the proposed antenna. (b) Modified circuit model of the proposed antenna.

4.2. Total Impedance

The total input impedance of the wide-band antenna with defected ground plane can be derived as

$$Z_{in} = \left[\frac{1}{(Z_{ml})} + \frac{1}{Z_c} + \frac{1}{Z_f} + \frac{1}{Z_s} + \frac{1}{Z_m} + \frac{1}{Z_p}\right] \tag{9}$$

The equivalent circuit model of the proposed Antenna3 is given in Figure 5(a) which is modified to Figure 5(b).

The Z_1, Z_2 and Z_3 impedances of the microstrip line are offered by the microstrip lengths l_1, l_2 and l_3, respectively, which are connected in series. It can be derived as

$$Z_{ml} = [Z_1 + Z_2 + Z_3] = \left[\left(\frac{R_1 + j\cdot\omega\cdot L_1}{G_1 + j\cdot\omega\cdot C_1}\right)^{1/2} + \left(\frac{R_2 + j\cdot\omega\cdot L_2}{G_2 + j\cdot\omega\cdot C_2}\right)^{1/2} + \left(\frac{R_3 + j\cdot\omega\cdot L_3}{G_3 + j\cdot\omega\cdot C_3}\right)^{1/2}\right] \tag{10}$$

The impedances of Z_c and Z_f are calculated as

$$Z_c = \frac{1}{j\cdot\omega\cdot C_c} \tag{11}$$

and

$$Z_f = \frac{1}{j\cdot\omega\cdot C_f} \tag{12}$$

The impedances Z_c and Z_f are offered by coupling capacitance (C_c) and fringing capacitance (C_f) between the two resonators defined in [24–27], respectively which are connected in parallel form with impedance of microstrip line as shown in Figure 5.

The input impedances of Z_p and Z_m are given as

$$Z_p = \frac{1}{\dfrac{1}{R_p} + j\,\omega C_p + \dfrac{1}{j\omega L_p}} \tag{13}$$

$$Z_m = \left(j\cdot\omega\cdot L_m + \frac{1}{j\cdot\omega\cdot C_m}\right) \tag{14}$$

where Z_p = impedance of the circular patch, Z_m = mutual impedance, L_m = mutual inductance, and C_m = mutual capacitance between two resonators (square slot and circular patch) circuits as shown in Figure 5 [27].

Now using Eq. (9), one can calculate various antenna parameters such as reflection coefficient, VSWR and return loss of the proposed antenna as

$$\Gamma = \frac{Z_{in} - Z_0}{Z_{in} + Z_0} \tag{15}$$

$$VSWR = \frac{1 + |\Gamma|}{1 - |\Gamma|} \tag{16}$$

and

$$RL = 20\log|\Gamma| \tag{17}$$

5. PARAMETRIC STUDY

A parametric study is first performed by changing the length (L_f), width (W_f) of the microstrip-fed-line and radius (r) of the circular patch under the square-shaped slot on the ground plane of the proposed Antenna3. These results are shown in Figures 6 to 11. Note that here in all these simulations the finite ground plane size is assumed to be $32 \times 32\,\text{mm}^2$ and square-shaped slot size $14.5 \times 14.5\,\text{mm}^2$. With decreasing L_f of the microstrip line, the higher resonance frequencies are shifted toward lower side whereas lower resonance frequencies remain almost constant. It is observed that with increasing the length (L_f) of the microstrip line, Antenna3 obtains dualband characteristics whereas lower and higher resonance frequencies are almost constant as shown in Figure 6.

Figure 7 shows the effect of varying width (W_f) of microstrip-line-fed on the return loss characteristics. From the figure, changing W_f of the Antenna3 achieved the dualband effect whereas the lower and upper resonance frequencies are almost constant. At the minimum value of W_f, Antenna3 improves the impedance bandwidth at the lower resonance compared to the upper resonance frequencies. Further at the 3.05 mm optimum value of W_f, the return loss deteriorates at some resonance frequencies as well as improves impedance bandwidth. So an optimum value of 3.05 mm has been considered in fabricated prototype.

The separation between the circular patch and the ground plane plays a crucial role in obtaining wider impedance bandwidth. Figure 8 shows the variation in return loss by varying the separation between the circular patch and finite ground plane. It can be seen from the figure that a minimum and maximum separation gives the dual and triple band operations at the higher frequencies, and the lower and upper resonance frequencies are almost constant. Hence, the separation needs to be optimized, and the optimum value is found to be 7.0 mm. At this optimum value, maximum coupling of electromagnetic energy between circular patch and square-shaped slot is achieved over a wide impedance bandwidth. Table 2 shows the effect on return loss and its impedance bandwidth of Antenna3.

The effect of varying the length (L_f) of microstrip-line-fed on axial ratio of the proposed Antenna3 is shown in Figure 9. From the figure, the three CP bands are obtained with decreasing the $L_f = 22.05$ mm whereas two CP bands are achieved with increasing L_f from 3.05 mm to 4.05 mm.

Figure 10 shows the effect of varying the width (W_f) of microstrip-line-fed on the axial ratio of the proposed Antenna3. From the figure, increasing and decreasing the W_f of the Antenna3 achieve the two CP bands at the lower and upper resonance frequencies respectively, and its corresponding 3 dB axial ratio bandwidths are decreased whereas upper resonance frequencies are almost constant. It is

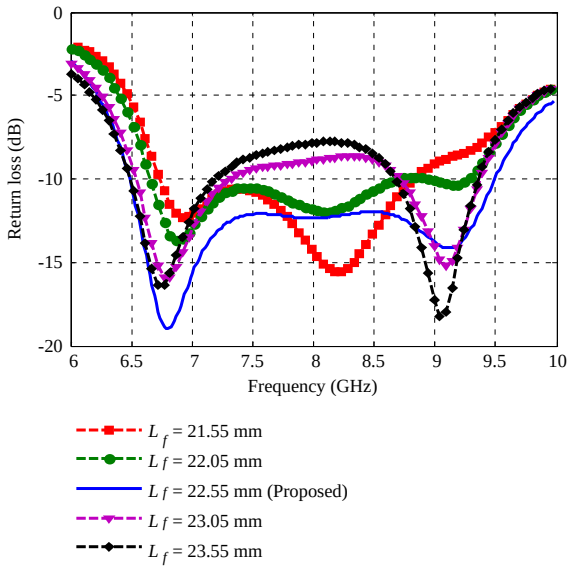

Figure 6. Variation of return loss for different values of length L_f.

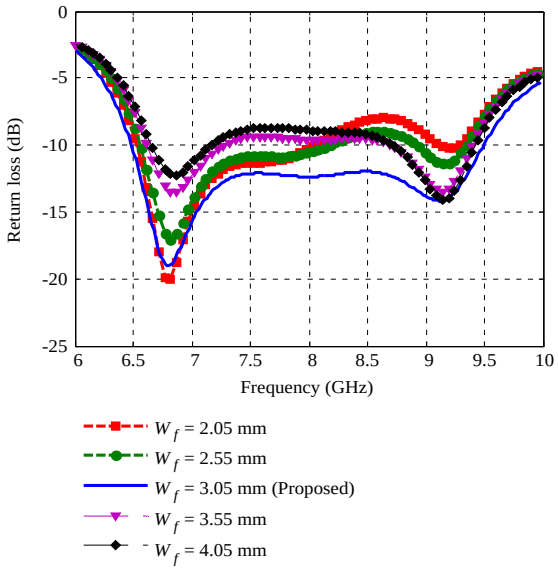

Figure 7. Variation of return loss for different values of width W_f.

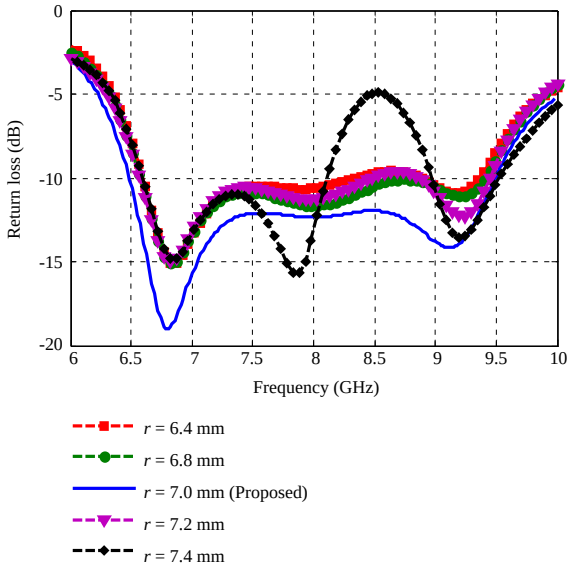

Figure 8. Variation of return loss for different values of radius (r).

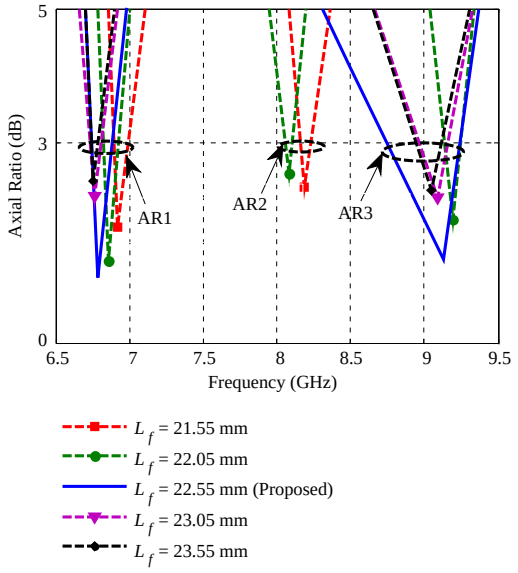

Figure 9. Variation of axial ratio for different values of length L_f.

Table 2. Calculated impedance bandwidth with the variation of L_f, W_f and r.

Variation of parameters (mm)	Lower frequency band		Upper frequency band	
	Frequency band (GHz)	BW (%)	Frequency band (GHz)	BW (%)
$L_f = 21.55$	(6.76–8.78)	25.99	NA	NA
$L_f = 22.05$	(6.66–8.68)	26.33	(8.99–9.29)	3.28
L_f = 22.55	**(6.48–9.50)**	**37.79**	**NA**	**NA**
$L_f = 23.05$	(6.56–7.32)	10.95	(8.73–9.36)	6.965
$L_f = 23.55$	(6.51–7.20)	10.06	(8.68–9.39)	7.858
$W_f = 2.05$	(6.55–8.03)	20.30	(9.09–9.24)	1.631
$W_f = 2.55$	(6.56–8.15)	21.61	(8.93–9.34)	4.480
W_f = 3.05	**(6.48–9.50)**	**37.79**	**NA**	**NA**
$W_f = 3.55$	(6.61–7.27)	9.51	(8.73–9.39)	7.282
$W_f = 4.05$	(6.66–7.17)	7.37	(8.73–9.44)	7.815
$R = 6.4$	(6.60–9.34)	34.37	NA	NA
$R = 6.8$	(6.56–9.39)	35.48	NA	NA
R = 7.0	**(6.48–9.50)**	**37.79**	**NA**	**NA**
$R = 7.2$	(6.56–9.44)	36	NA	NA
$R = 7.4$	(6.60–8.10)	20.40	(8.90–9.54)	6.94

realized that the optimum is obtained at $W_f = 3.05$ mm with two CP bands.

Figure 11 shows the effect of varying the radius (r) of circular patch on the axial ratio of the proposed Antenna3. From the figure, with increasing and decreasing the 'r', Antenna3 achieves the three CP bands at the lower, middle and upper resonance frequencies respectively, and its corresponding 3 dB axial ratio bandwidths are decreased whereas all resonance frequencies are almost constant. Finally, it can be seen from the figure that Antenna3 achieves a better axial ratio bandwidth at optimum values of $L_f = 22.55$ mm, $W_f = 3.05$ mm and $r = 7.0$ mm with two and three CP bands. The effect on the axial ratio bandwidth (ARBW) of the different CP bands for the proposed Antenna3 is shown in Table 3.

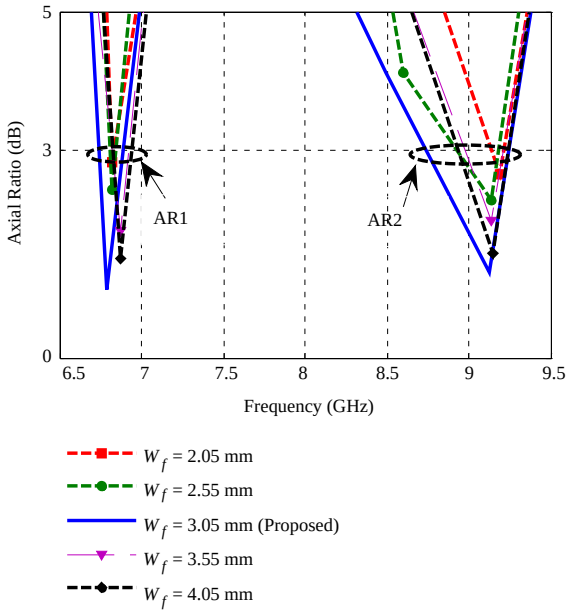

Figure 10. Variation of axial ratio for different values of width W_f.

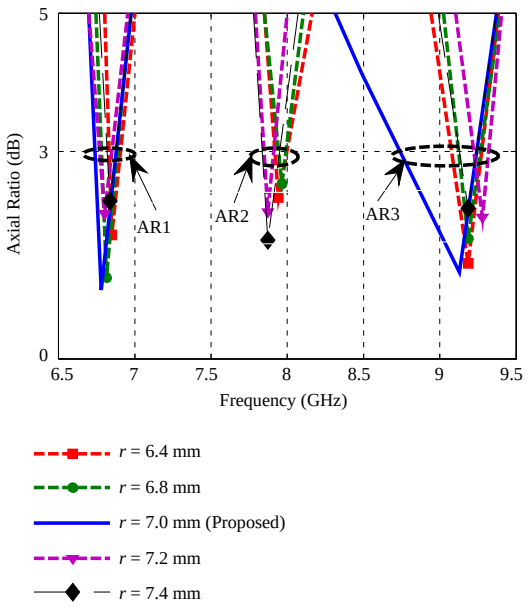

Figure 11. Variation of axial ratio for different values of radius r.

Table 3. Calculated ARBW with the variation of L_f, W_f and r.

Variation of parameters (mm)	AR1		AR2		AR3	
	Frequency band (GHz)	ARBW (%)	Frequency band (GHz)	ARBW (%)	Frequency band (GHz)	ARBW (%)
$L_f = 21.55$	(6.90–7.05)	1.43	(8.10–8.25)	1.834	NA	NA
$L_f = 22.05$	(6.82–6.93)	1.6	(7.97–8.10)	1.617	(9.12–9.20)	0.873
L_f = 22.55	**(6.72–6.89)**	**2.79**	**NA**	**NA**	**(8.73–9.22)**	**5.459**
$L_f = 23.05$	(6.73–6.81)	1.256	NA	NA	(8.96–9.18)	2.42
$L_f = 23.55$	(6.73–6.80)	1.034	NA	NA	(8.93–9.12)	2.105
$W_f = 2.05$	(6.79–6.81)	0.294	NA	NA	(9.15–9.25)	1.086
$W_f = 2.55$	(6.76–6.84)	1.176	NA	NA	(8.92–9.18)	2.872
W_f = 3.05	**(6.72–6.89)**	**2.79**	**NA**	**NA**	**(8.73–9.22)**	**5.459**
$W_f = 3.55$	(6.82–6.92)	1.455	NA	NA	(8.99–9.25)	2.774
$W_f = 4.05$	(6.82–6.94)	1.741	NA	NA	(8.92–9.21)	3.199
$R = 6.4$	(6.84–6.92)	1.162	(7.92–8.12)	2.493	(9.09–9.28)	2.060
$R = 6.8$	(6.76–6.89)	1.88	(7.95–8.12)	2.115	(9.13–9.26)	1.413
R = 7.0	**(6.72–6.89)**	**2.79**	**NA**	**NA**	**(8.73–9.22)**	**5.459**
$R = 7.2$	(6.76–6.86)	1.468	(7.84–7.92)	1.015	(9.24–9.32)	0.862
$R = 7.4$	(6.89–6.99)	1.440	(7.82–7.95)	1.648	(9.13–9.22)	0.981

6. DISCUSSION OF RESULTS

The proposed Antenna3 is designed and simulated by the IE3D software based on method of moment (MoM) [28] and fabricated with optimized dimensions as given in Table 1. In Figure 12, there are slightly variations in theoretical, simulated and measured return loss curves due to fabrication constrains, uncertainties in the dielectric constant, substrate thickness, soldering effects and the quality of the SMA connector. Figure 13 shows the fabricated prototype of the proposed microstrip-line-fed Antenna3 with defected ground structure. The measurement results are performed by vector analyzer Agilent N5230A.

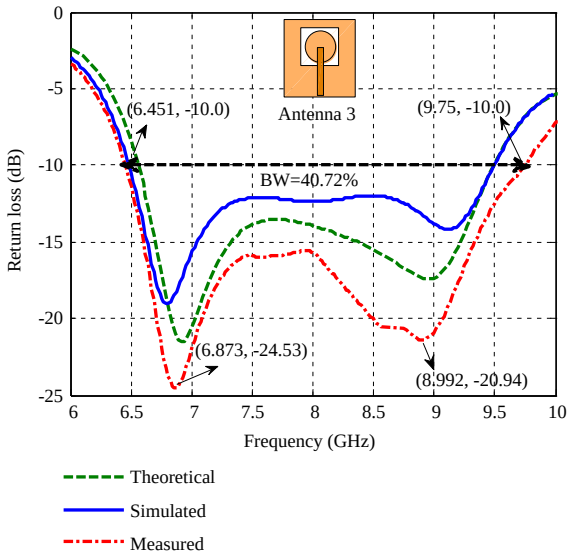

Figure 12. Plot of return loss versus frequency for proposed Antenna3.

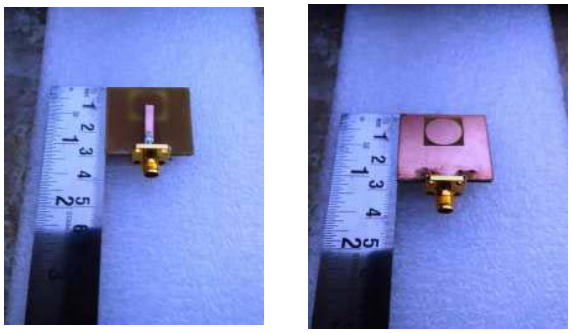

Figure 13. Photograph of the fabricated Antenna3. (a) Top view. (b) Bottom view.

Table 4. Performance comparison between the proposed antenna and some existing antenna.

S. No.	Reference	Antenna Size (mm^2)	Frequency band (GHz)	Bandwidth (%)	Gain (dBi)	Applications
1	[13] 2013	32×32	(9.35–10.55)	12.2	8.7	X-band
2	[14] 2014	30×30	(4.04–7.28)	60.3	3	C-band
3	[15] 2014	21×30	(6.8–7.3)	7.09	5.54	C and X-band
4	[16] 2014	20×17.2	(8.69–9.14)	5.02	4.45	X-band
5	**Proposed antenna**	**32×32**	**(6.48–9.5)**	**37.79**	**8.281**	**C and X-band**

The theoretical and simulated results are shown along with measured ones for designed Antenna3 in Figure 12. From this figure, it is found that the dual resonance frequencies occur at 6.942 GHz and 8.801 GHz. These closely spaced dual resonating frequencies are combined to provide wider impedance bandwidth. The frequency band of operation is obtained from 6.652 GHz to 9.35 GHz for return loss value less than −10 dB which covers the C- and partially X-band operation. Antenna3 shows impedance bandwidths of 40.72% (measured), 37.79% (simulated) and 36.77% (theoretical). The simulated and measured results are in good agreement with theoretical analysis.

In addition, various antennas with defected ground plane are previously reported [13–16] to involve in complex calculation and sophisticated design structure as compared to the proposed antenna. A detailed comparison in terms of parameters, such as antenna size, total area occupied by the antenna, bandwidth, gain and its frequency of operation, has been summarized in Table 4. This innovates us to work on wide-band microstrip line-fed antenna with defected ground structure which can overcome the above limitations.

The comparative plots of gain versus frequency for Antenna1, Antenna2 and proposed Antenna3 are shown in Figure 14. From the figure, it is clearly observed that the gain varies from 2.4 dBi to 4.1 dBi over an operating frequency range of 6.5 GHz to 7.95 GHz for Antenna1, and the gain varies from 4.2 dBi to 5.74 dBi over an operating frequency range of 6.55 GHz to 9.15 GHz for Antenna2, whereas, gain of Antenna3 varies from 3.94 dBi to 6.63 dBi over an operating frequency range of 6.48 GHz to 9.5 GHz. The maximum peak gains are obtained, 5.384 dBi, 6.716 dBi and 8.281 dBi at the higher resonance frequency.

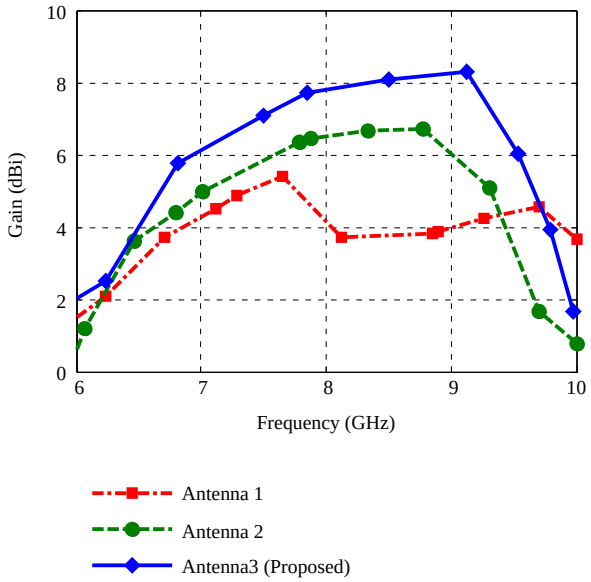

Figure 14. Comparative plot of gain versus frequency for Antenna1, Antenna2 and proposed Antenna3.

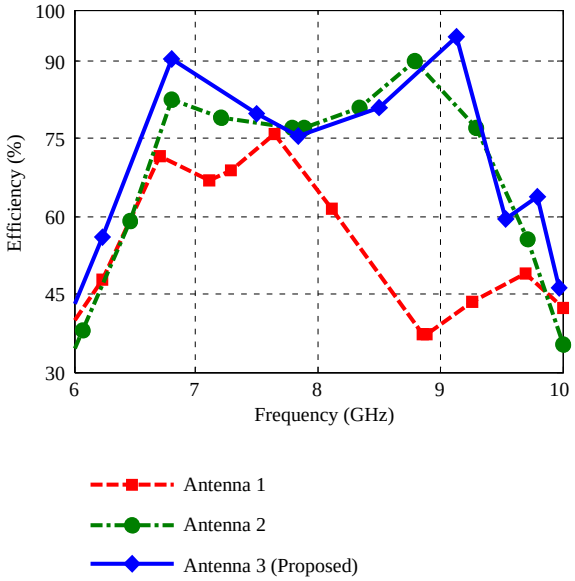

Figure 15. Comparative plot of efficiency versus frequency for Antenna1, Antenna2 and proposed Antenna3.

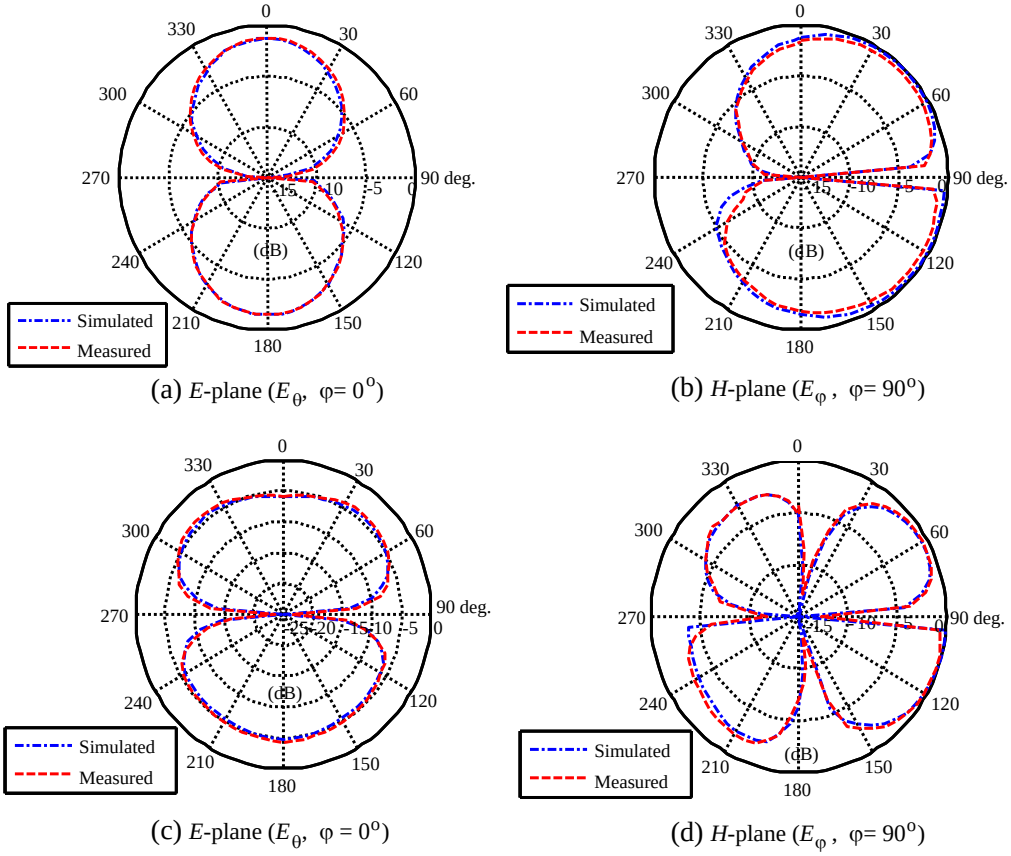

(a) *E*-plane (E_θ, $\varphi = 0^o$)

(b) *H*-plane (E_φ, $\varphi = 90^o$)

(c) *E*-plane (E_θ, $\varphi = 0^o$)

(d) *H*-plane (E_φ, $\varphi = 90^o$)

Figure 16. Radiation patterns of E and H plane for Antenna3, (a), (b) at 6.806 GHz and (c), (d) at 9.13 GHz.

Table 5. Comparative study of the Antenna1, Antenna2 and proposed Antenna3.

DGS antennas	Frequency band (GHz)	Bandwidth (%)	Peak Gain (dBi)	Max. Efficiency (%)	Applications
Antenna1	(6.5–7.95)	20.06	5.384	75.98	C- band
Antenna2	(6.55–9.15)	33.12	6.716	90.05	C and X- band
Proposed Antenna3	**(6.48–9.5)**	**37.79**	**8.281**	**94.77**	**C and X-band**

The comparative plot of the antenna efficiency with frequency for Antenna1, Antenna2 and Antenna3 is shown in Figure 15. For Antenna1 it is found that the efficiencies are 71.7% at 6.711 GHz and 75.98% at 7.651 GHz. From the figure it can be seen that the efficiencies are obtained as 82.76% (at 6.795 GHz) and 90.05% (at 8.771 GHz) for Antenna2, whereas, Antenna3 achieves the maximum antenna efficiencies which are 90.43% and 94.77% at the lower (6.806 GHz) and upper (9.13 GHz) resonance frequencies, respectively. It is noticed that maximum efficiency is obtained at the upper resonance frequency. Antenna3 gives a better performance than Antenna1 and Antenna2. The comparative performance of Antenna1, Antenna2 and Antenna3 is shown in Table 5.

The E- and H-plane radiation patterns of the proposed Antenna3 at the lower and upper resonance frequencies are shown in Figure 16. Figures 16(a)–(d) show radiation patterns of Antenna3 for E_θ, $\varphi = 0^\circ$ at 6.942 GHz and E_φ, $\varphi = 90^\circ$ at 6.942 GHz, E_θ, $\varphi = 0^\circ$ at 8.801 GHz and E_φ, $\varphi = 90^\circ$ at 8.801 GHz, respectively. It is found that measured results of the radiation pattern are in good agreement with simulated ones. It is observed that H-plane radiations of the proposed Antenna3 are nearly the same, in spite of difference in radiated power. Similarly, the results are analyzed for E-plane radiation pattern and achieve a better beamwidth of Antenna3. The proposed Antenna3 achieves a bidirectional radiation pattern due to effect of finite ground structure.

7. CONCLUSION

In this article, a new microstrip-line-fed antenna with defected ground structure is designed and fabricated. Antenna3 analyzed by equivalent circuit model for microstrip line with DGS is presented. The measured impedance bandwidth 40.72% at frequency band (6.45 GHz–9.75 GHz) is obtained. The 3 dB axial ratio bandwidths (ARBW) 2.79% and 5.459% for dual resonance frequencies are presented. A compact size of $32 \times 32\,\text{mm}^2$ is obtained. Bidirectional patterns with maximum efficiency and peak gains are obtained at higher resonance frequency. For applications, the frequency responses of the proposed Antenna3 are covered in the frequency bands of C and X operations. The effect of the defected parameters of DGS on performance is also examined. The measurement shows good consistency with the simulated and theoretical analysis.

REFERENCES

1. Kumar, G. and K. P. Ray, *Broadband Microstrip Antennas*, Artech House, Boston, 2003.
2. Wu, C.-M., J.-W. Syu, and W.-C. Liu, "Dual-band slotted patch antenna with defective ground for WLAN/WiMAX applications," *Progress In Electromagnetics Research Letters*, Vol. 53, 1–6, 2015.
3. Gautam, A. K. and B. K. Kanaujia, "A novel dual-band asymmetric slit with defected ground structure microstrip antenna for circular polarization operation," *Microwave and Optical Technology Letters*, Vol. 55, 1198–1201, 2013.
4. Nasimuddin, X. Qing, and Z. N. Chen, "Compact asymmetric-slit microstrip antennas for circular polarization," *IEEE Transactions on Antennas and Propagation*, Vol. 59, 285–288, 2011.
5. Guha, D., S. Biswas, M. Biswas, J. Y. Siddiqui, and Y. M. M. Antar, "Concentric ring-shaped defected ground structure for microstrip application," *IEEE Antennas and Wireless Propagation Letters*, Vol. 5, 402–405, 2006.

6. Wang, T., Y.-Z. Yin, J. Yang, Y.-L. Zhang, and J.-J. Xie, "Compact triple-band antenna using defected ground structure for WLAN/WiMAX applications," *Progress In Electromagnetics Research Letters*, Vol. 35, 155–164, 2012.
7. Pei, J., A.-G. Wang, S. Gao, and W. Leng, "Miniaturized triple-band antenna with a defected ground plane for WLAN/WiMAX applications," *IEEE Antennas and Wireless Propagation Letters*, Vol. 10, 298–301, 2011.
8. Das, S., P. P. Sarkar, and S. K. Chowdhury, "Design and analysis of a compact triple band slotted microstrip antenna with modified ground plane for wireless communication applications," *Progress In Electromagnetics Research B*, Vol. 60, 215–225, 2014.
9. Zhang, L., B. Chen, Y.-C. Jiao, and Z.-B. Weng, "Compact triple-band monopole antenna with two strips for WLAN/WiMAX applications," *Microwave and Optical Technology Letters*, Vol. 54, 2650–2653, 2012.
10. Samsuzzaman, M., M. T. Islam, J. S. Mandeep, and N. Misran, "Printed wide-slot antenna design with bandwidth and gain enhancement on low-cost substrate," *The Scientific World Journal*, Vol. 14, 1–10, 2014.
11. Fu, S.-H. and C.-M. Tong, "A novel CSRR-based defected ground structure with dual-bandgap characteristics," *Microwave and Optical Technology Letters*, Vol. 51, 2908–2910, 2009.
12. Kumar, K. M., B. K. Kanaujia, S. Dwari, S. Kumar, and A. K. Gautam, "Analysis and design of wide band microstrip-line-fed antenna with defected ground structure for Ku band applications," *International Journal of Electronics and Communications*, Vol. 68, 915–957, 2014.
13. Abhishek, K., R. Sharma, and S. Kumar, "Bandwidth enhancement using Z-shaped defected ground structure for a microstrip antenna," *Microwave and Optical Technology Letters*, Vol. 55, 2251–2254, 2013.
14. Rawat, S. and K. K. Sharma, "A compact broadband microstrip patch antenna with defected ground structure for C-band applications," *Central European Journal of Engineering*, Vol. 4, 287–292, 2014.
15. Mourad, M. and M. Essaaidi, "A dual ultra wide band slotted antenna for C and X-band application," *Progress In Electromagnetics Research Letters*, Vol. 47, 91–96, 2014.
16. Samsuzzaman, M. and M. T. Islam, "Inverted S-shaped compact antenna X-band applications," *The Scientific World Journal*, Vol. 14, 1–11, 2014.
17. Garg, R., P. Bhartia, I. Bahl, and A. Ittipiboon, *Microstrip Antenna Design Handbook*, Artech House, Boston, 2001.
18. Collins, R. E., *Foundations of Microwave Engineering*, John Wiley & Sons, 2001.
19. Abboud, F., J. P. Damiano, and A. Papiernik, "A new model for calculating the input impedance of coax-fed circular microstrip antennas with and without air gaps," *IEEE Transactions on Antennas and Propagation*, Vol. 38, 1882–1885, 1990.
20. Pozar, D. M., *Microwave Engineering*, John Wiley & Sons, 2005.
21. Huang, Y. I. and K. Boyle, *Antenna from Theory to Practice*, John Wiley & Sons, 2008.
22. Kominami, M., D. M. Pozar, and D. H. Schaubert, "Dipole and slot elements and array on semi-infinite substrate," *IEEE Transactions on Antennas and Propagation*, Vol. 33, 600–607, 1985.
23. Balanis, C. A., *Antenna Theory Analysis and Design*, John Wiley & Sons, 2005.
24. Lu, J. H., C. L. Tang, and K. L. Wong, "Single feed slotted equilateral triangular microstrip antenna," *IEEE Transactions on Antennas and Propagation*, Vol. 47, 1174–1178, 1999.
25. Kirschning, M., R. H. Jansen, and N. H. L. Koster, "Accurate model for open and effect of microstrip lines," *Electron. Letters*, Vol. 17, 123–125, 1981.
26. Wolf, E. A., *Antenna Analysis*, Artech House, 1988.
27. Terman, F. E., *Electronic and Radio Engineering*, McGraw-Hill, 1995.
28. IE3D Simulation Software, Version 14.05, Zeland software Inc., USA, 2008.